2-8-2000

Pion-induced transport of π mesons in nuclei

S. G. Mashnik

R. J. Peterson

A. J. Sierk

Michael R. Braunstein

Pion-induced transport of π mesons in nuclei

S. G. Mashnik,[1,]* R. J. Peterson,[2] A. J. Sierk,[1] and M. R. Braunstein[3]

[1]*T-2, Theoretical Division, Los Alamos National Laboratory, Los Alamos, New Mexico 87545*
[2]*Nuclear Physics Laboratory, University of Colorado, Boulder, Colorado 80309*
[3]*Physics Department, Central Washington University, Ellensburg, Washington 98926*

A large body of data for pion-induced neutral pion continuum spectra spanning outgoing energies near 180 MeV shows no dip there that might be ascribed to internal strong absorption processes involving the formation of Δ's. This is the same observation previously made for the charged pion continuum spectra. Calculations in an intranuclear cascade model or a cascade exciton model with free-space parameters predict such a dip for both neutral and charged pions. We explore several medium modifications to the interactions of pions with internal nucleons that are able to reproduce the data for nuclei from ^{7}Li through Bi.

I. INTRODUCTION

Continuum spectra of π mesons have been used to diagnose the mechanisms of many high-energy nuclear reactions. Since these mesons are themselves involved with the nuclear field, their production and propagation within nuclei may be much more complex than is the case in free space. Δ's, readily produced by and decaying to pions, are also important participants in nuclear reactions, with a strong role in sharing energy. At high beam energies other baryon states may also participate in nuclear reactions.

The simplest pion continuum spectra are those produced by electromagnetic or pion beams. Those from pion beams can include $(\pi,2\pi)$ mechanisms yielding two strongly interacting bosons, which may be correlated. These correlations would also be present among the many pions produced in relativistic heavy ion collisions, but should be easier to understand in pion-induced continuum spectra. Such continuum spectra should show a self-absorption dip near kinetic energies of 180 MeV, as the pions form Δ's and are absorbed or rescattered. It was a surprise to find this feature lacking in the spectra of charged pions [no charge exchange (NCX) scattering] resulting from 500 MeV pion beams [1]. At this pion energy, the beam particles have a long mean free path in nuclei, and can participate in πN reactions throughout much of the nuclear volume. Particles with shorter mean free paths can thus be created at interesting densities.

A classical cascade with quantum corrections reaction model [2] also showed the self-absorption dip for these NCX reactions, in disagreement with the data. It was found that forbidding pions resulting from pion-induced pion production from interacting for a time of 2 fm/c removed the self-absorption, and yielded much superior agreement with the data [1]. This can be taken as a sign of a new and important feature of pions in nuclei, perhaps related to the presence of two pions. Another transport model, using the Boltzmann-Uehling-Uhlenback (BUU)/ART formalism, found less of an absorption dip near 180 MeV, but also failed to account for

the NCX data at angles forward of 90° by a factor of 2 [3]. Comparisons of calculations to data will be summarized in Sec. V below.

In the present work we present corresponding continuum spectra for neutral pions [from single charge exchange (SCX) scattering] for several beam energies extending to larger energy losses (lower outgoing kinetic energies), and for a wider range of nuclear targets than was used for the NCX work. Inclusion of a wide range of target masses gives new sensitivity to the surface-to-volume ratio, or to a range of length scales over which interactions may or may not occur. The means of measuring neutral pion spectra is very different from the use of a magnetic spectrometer for charged pions, and this difference demonstrates a valuable consistency check on the results. The elementary πN cross sections near 500 MeV have much the same angular dependence for SCX and NCX processes.

The SCX data are compared to spectra computed with the intranuclear cascade (INC) model through the code used in Ref. [1], and through another method [4], used in the cascade-exciton model (CEM) [5]. These theoretical models are also used for comparisons to the NCX data for consistency. The π^0 spectra from this work also show no self-absorption dip, and again calculations using what is known from free space fail to match the data.

II. EXPERIMENTAL METHODS

This work reports SCX spectra from three separate experiments. A beam energy of 475 MeV (600 MeV/c) was used in a search for SCX to excite Δ's directly in nuclei [6]. A study at 467 MeV (590 MeV/c) used a wider range of target nuclei and angles [7]. At 400 and 500 MeV (522 and 625 MeV/c), the quasielastic portion of the continuum SCX spectra was measured, with energy spectra extending down to near 180 MeV [8,9]. All experiments used the same π^0 detector and pion beam line.

Pion beams were provided by the LAMPF P^3 beam line, with beam monitoring by use of a calibrated ion chamber and by the intensity of the primary proton beam on the production target. Beam energies are known to an accuracy of 5

TABLE I. Angle settings for the two crates of the π^0 spectrometer, with their central and mean angle and energy acceptances, as used for the several parts of the present study. Scattering angles were in the horizontal plane, with opening angles η in a vertical plane. At the 90 cm radius R used for most spectra with large energy losses the spectrometer accepted events in a scattering range of $\pm 9°$ about the mean angle. The 0°, 190 MeV setting was used for normalization runs with 160 MeV π^- on hydrogen [6,7].

Nominal angle (deg)	Mean angle (deg)	Nominal energy (MeV)	Nominal η (deg)	Radius, R (cm)
Pion kinetic energy 467 MeV [a] and 475 MeV [b]				
0	8.5	70	82.3	90
0	8.5	130	61.3	90
0	8.5	190	49.1	90
25	26	70	82.3	90
25	26	130	61.3	90
25	26	190	49.1	90
50	50	70	82.3	90
50	50	130	61.3	90
50	50	190	49.1	110
Pion kinetic energy 400 MeV [c]				
62.6	62.5	250	41.05	80
Pion kinetic energy 500 MeV [d]				
0	5.3	350	32.3	140
30	30.3	350	32.3	140
50	50.1	350	32.3	110
70	70.1	270	38.9	100
88.8	89.6	225	44.0	80

[a]Reference [6].
[b]Reference [7].
[c]Reference [8].
[d]Reference [8].

MeV, with momentum spreads variously between 0.5 and 0.8%. An achromatic beam tune was used, in contrast to the dispersed beams from the P^3 line used for the NCX spectra.

Neutral pions were detected by the LAMPF π^0 spectrometer, comprised of two detector modules (''crates''), each of lead glass converters to generate electromagnetic showers from the π^0 decay photons, wire chambers to locate the centroids of those showers, and arrays of lead glass as calorimeters. A more complete description is found in [6]; the arrangement of Ref. [7] was the same, and that used for 400 and 500 MeV beams is described in [8]. Measurement of the opening angle between the two decay photons and of the total energy E can be combined to compute the invariant mass of the decay particle and its laboratory energy. The opening angle between the crates was varied to capture decays from neutral pions, with several settings used to determine the continuum spectra for low energies. One opening sufficed for coverage of the quasielastic region. Crate angles could be chosen to capture π^0's at a given laboratory scattering angle. The list of settings used for the three studies treated in this work is given in Table I. A substantial overlap of spectra from each setting was employed to ensure match-

ing and consistency in the spectra.

Crate angles were set to collect outgoing π^0 events at the energies listed in Table I using an energy sharing $X = (E_1 - E_2)/(E_1 + E_2)$ of zero, where E_1 and E_2 are the energies of the two photon events. Events for which X was not above 0.40 were used for the final spectra, since energy resolution was not an important goal for these continuum spectra. The fiducial volume of the calorimeters used for acceptable events was also increased for better statistical accuracy. Cross sections obtained under the more generous conditions agreed with those taken for more standard conditions, after appropriate Monte Carlo corrections, to within 5%.

Targets were CH_2, CD_2, ^7Li (99%), C, Fe, ^{90}Zr (98%), and Bi. Attenuation corrections as large as 50% were required for photons exiting the Bi target; uncertainties in these corrections were within 10% for this, the most affected of
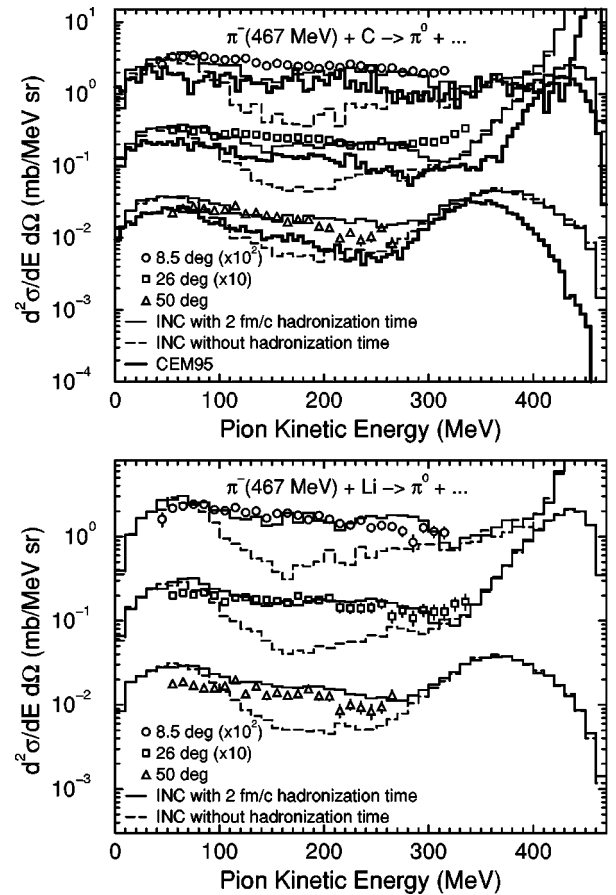

FIG. 1. Measured energy spectra for neutral pions from 467 MeV π^- on a carbon and ^7Li targets, using the settings of the Pizero Spectrometer as listed in Table I [7]. INC calculations using free-space interactions as for the NCX spectra published in Ref. [1] are shown by the dashed histograms. The heavy solid histograms show CEM spectra, using the same assumptions for the interactions but with a different computational method as described in the text. Note the self-absorption dip predicted near 180 MeV but absent in the data. INC calculations that forbid pions from $(\pi, 2\pi)$ reactions from interacting for a time of 2 fm/c are shown by the light solid histograms, filling the dip as also found previously for the NCX continuum spectra [1]. Cross sections, energies, and angles are all in the laboratory reference frame for these and other spectra.

our data cases at 49% of a radiation length for the target thickness.

A Monte Carlo code (PIANG) [10] was used to determine the acceptance of the spectrometer, as presented in many previous works [11]. This was tested in the present case by use of a 160 MeV π^- beam on proton targets, where the single charge exchange cross sections are known. The magnitude and angular dependence expected [12] were obtained in our analysis. For the beam energies used to generate the quasielastic continuum spectra, the acceptance was also checked or calibrated from measurements of the $p(\pi^-,\pi^0)n$ reaction, and comparison to standard SCX cross sections [12]. The hydrogen target was used as a CH_2 disk of the same size as the other complex targets, with appropriate subtraction of events from a matched carbon disk. The absolute scale of the π^0 spectra from π^- beams was determined to 13%. The energy resolution obtained in all three experiments agreed well with the results of PIANG for the experimental conditions used. The energy resolution of the π^0 spectra was 11 MeV near outgoing π^0 energies of 160 MeV.

The invariant mass distribution determined from these observations showed a clean π^0 peak, centered near 135 MeV and with a full width at half maximum of 50 MeV, in agreement with the predictions of PIANG. A test on this spectrum ensured that single π^0 spectra were being measured.

Normalization for the π^+ beams was taken from an assumed charge symmetry for both charged beams on deuterium, where a solid CD_2 target of the same dimensions as those for CH_2 and C is used. π^0 spectra for the two beam states may be compared to an accuracy of 10%.

The dominant feature of these continuum spectra is the quasielastic SCX peak, formed by the incoherent reactions on individual nucleons within the complex nuclei. These results have been presented and compared to an eikonal nuclear reaction model [13] and to the computed role of nuclear interactions [14]. The present work focuses on the lower energy range of those spectra, and on previously unpublished data extending to very low laboratory energies for the π^0. Tables of data may be found in Refs. [7,8].

An example of the spectra obtained is shown in Fig. 1. The first point to be noted is the lack of a dip near pion lab energies of 180 MeV, exhibiting just the same feature noted in the NCX spectra [1].

III. THEORETICAL MODELS

Two models for the nuclear reactions of intermediate energy π mesons with complex nuclei are used, with or without modifications from the processes known in free space, to compute theoretical SCX and NCX continuum pion spectra.

The INC model of Gibbs and Kaufmann [2] is used here to compute π^0 spectra for $\pi^- + C$, in just the same fashion that this model was used for the NCX data [1]. This model uses elementary πN cross sections, including realistic models for pion production. The Pauli exclusion principle is applied to block recoil nucleons from πN collisions by requiring recoil nucleons to have some minimum energy. Short-range correlations among the target nucleons are included. This is a classical transport calculation in time intervals,
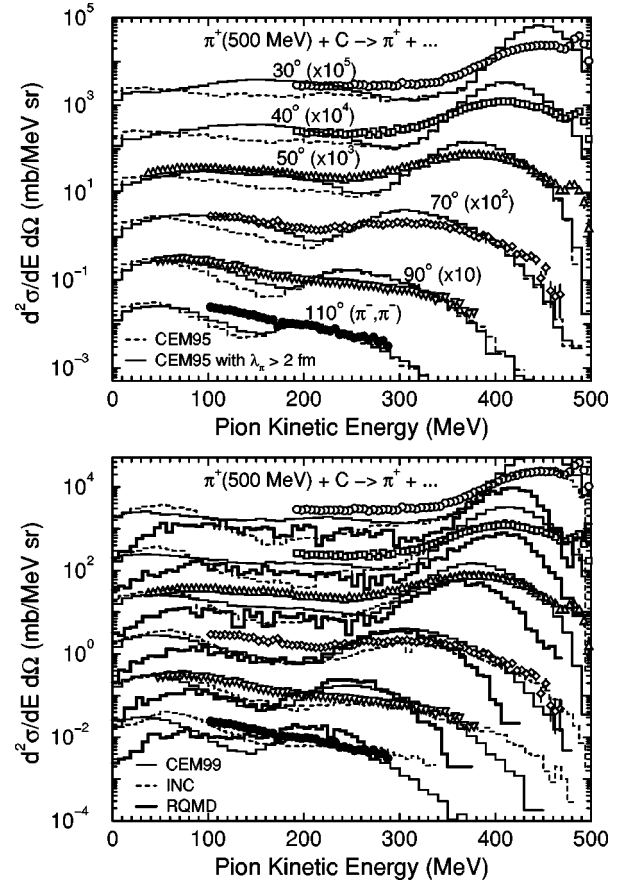

FIG. 2. Measured pion NCX spectra for 500 MeV π^+ on carbon [1] are compared to INC calculations from [1] by the dashed histograms on the bottom plot, without medium modifications. CEM calculations without (dashed histograms) and with (solid histograms) a 2 fm hadronization length for pions from $(\pi,2\pi)$ reactions are shown on the top plot. The solid histograms labeled as CEM99 on the bottom plot are calculated with a recent improved version of the CEM [18] without medium modifications. The heavy histograms show the calculations with the RQMD code [23] from Ref. [24].

meaning that local nucleon density effects are not included explicitly. The cascade proceeds by summing the incoherent effects of individual πN scatterings, and subsequent NN scatterings. The distribution of nucleons is computed from a sum of individual shell-model wave functions, while the pions sense no mean-field potential.

An extended version [15] of the cascade-exciton model (CEM) [5] is also used to compute NCX, SCX, and double charge exchange (DCX) continuum pion spectra. The DCX work will be presented elsewhere. This model and its computer code have been compared with good success to many reactions, at many energies, on a wide range of nuclear targets [16]. Only the pion SCX and NCX results are presented here. In the CEM, it is assumed that reactions occur in three stages. The first is the INC of the incident and other fast elementary particles. The excited nucleus that remains then emits preequilibrium ejectiles, followed by an evaporative third stage. Only the first stage is relevant to the pion spectra, although this model has also been applied to neutron, proton,
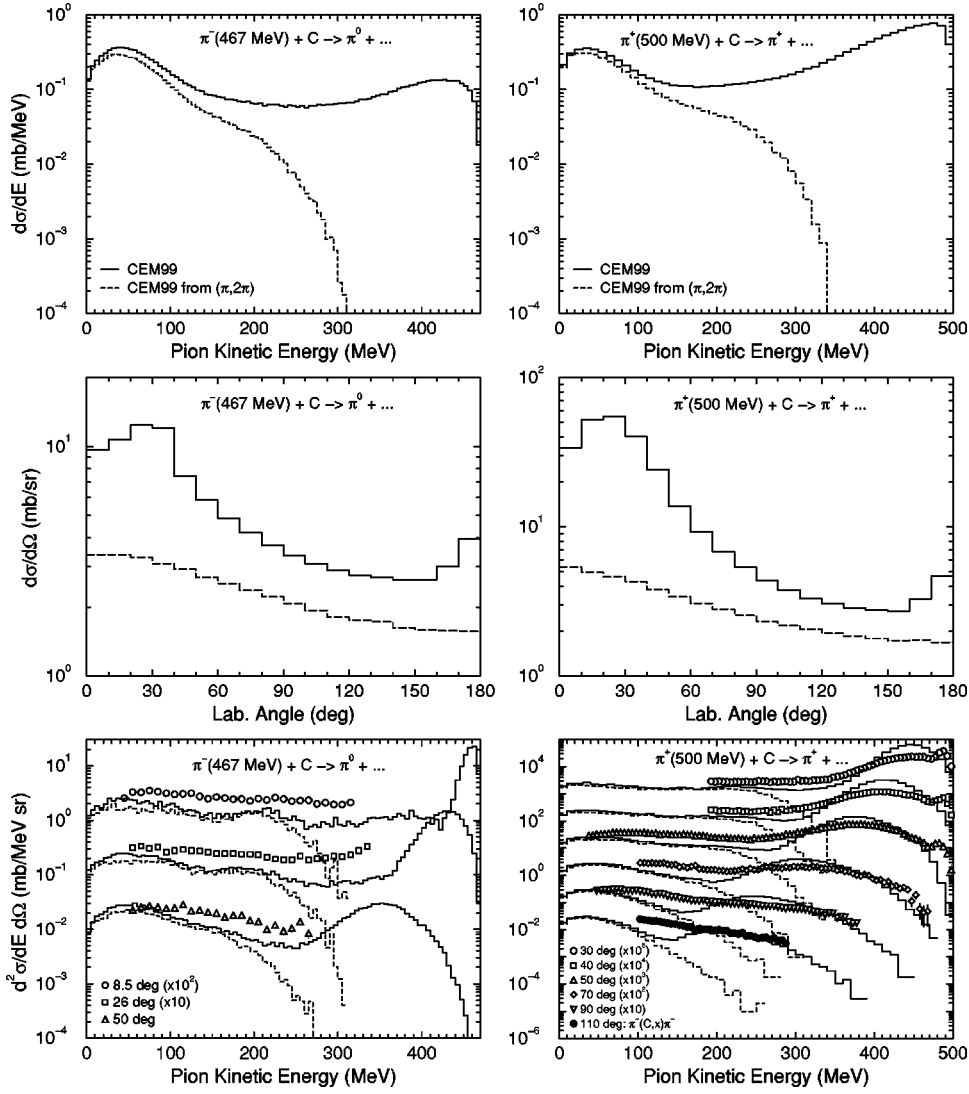
FIG. 3. Contributions from the pion production mode $(\pi,2\pi)$ to the total energy, angular, and double-differential NCX and SCX pion spectra as predicted by the CEM. Its integral yield is 24% for NCX at 500 MeV and 47% for SCX at 467 MeV of the total pion production cross sections, but these percentages change significantly both with the energy and the angle of the detected pions.

and complex particle spectra resulting from pion beams, involving all three stages [17].

The cascade stage of the CEM uses the Dubna INC model [4]. Nucleon distributions are taken from the functional forms found by electron scattering, with nucleon size effects removed. The momentum distribution of these nucleons is taken to be that of a Fermi gas at the local density. For simplicity, instead of using a continuous density distribution for the calculations, each nucleus is divided into seven concentric spheres with constant density inside each shell between spheres. A mean-field potential may be applied to the incoming pion projectiles, but changing this from 0 to 25 MeV (attractive) makes no more than a 20% effect on the continuum spectra near 180 MeV for our bombarding energies (see, e.g., [18]). The cascade proceeds by a series of incoherent elementary πN (and NN) interactions, using polynomial approximations to represent the actual experimental scattering distributions in angle and outgoing momentum. The elementary cross sections are taken from [4] for histograms labeled CEM95; more recent πN and NN cross sections [18] are used to generate the histograms labeled CEM97 and CEM99. Differences are neglible for the

π^0 continuum spectra. We include effects of the Pauli principle by forbidding interactions leading to final-state nucleons with a momentum less than the local Fermi momentum. At the boundaries between the concentric shells of nucleons of different densities, nucleons and pions should undergo classical refractions and reflections. These are not included in these calculations; instead straight line trajectories are continued at the boundaries, although energy is still conserved. If we include refraction effects using the method of Iljinov [19], the SCX continuum spectrum at 180 MeV changes by no more than 10%. Our model also ignores the effect of the depletion of local density for subsequent stages of the reaction due to the emission of nucleons; however this effect has been shown to be unimportant at energies below 1 GeV, even for light nuclei [4,20]. All the parameter values used in these CEM calculations can be found in Ref. [15].

Because of its importance in the processes under investigation, we discuss in a little more detail how the interaction of a pion with a nucleon is modeled in the CEM. At each point, a local mean free path proportional to the inverse of the product of the local density and the total free-space πN cross section is determined. A point of interaction is ran-
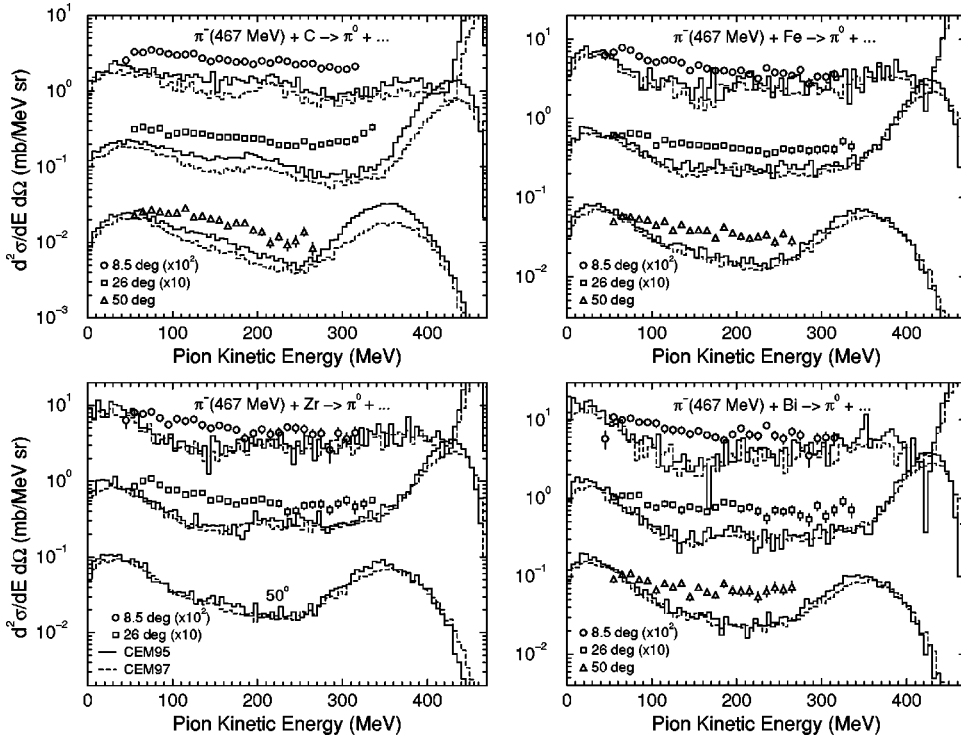
FIG. 4. Measured π^0 spectra for 467 MeV π^- beams on several targets [7] are compared to CEM calculations without medium modifications which use two different data sets for the elementary πN interactions. Differences in the calculated results are small.

domly determined along the projection of the pion momentum vector. At that point, the randomly directed Fermi momentum of the nucleon and the type of interaction are determined: (quasi)elastic scattering of the pion, charge exchange reaction, absorption, or pion production (inelastic). The probability of each type of interaction is calculated from the ratio of the experimental partial cross section at that πN center-of-mass energy to the total πN cross section. Suppose that choice happens to be a $(\pi, 2\pi)$ reaction. The final momenta of all the particles are chosen randomly from approximations to the experimental distributions for this reaction. Finally, if the nucleon momentum does not lie inside the local Fermi momentum sphere, the collision is accepted, and the cascade proceeds with each of the final particles interacting until absorbed or leaving the nucleus.

We must distinguish between two different processes which are both called ''absorption.'' Explicit pion absorption on two nucleons is included in the CEM by choosing randomly the two momenta from the Fermi-gas distribution of nucleons and applying known quasideuteron absorption cross sections to the resulting three-body system, again ensuring satisfaction of the exclusion principle. We account for the observed pion absorption on finite nuclei by using an effective number of four deuterons for all targets [21,22]. Changing this empirical normalization from one to four changes the calculated carbon SCX continuum spectrum near 180 MeV by no more than 15%. The second process, to which we have been referring to loosely as ''self absorption,'' involves the interaction of a pion with a single nucleon to form a Δ, which subsequently decays into a nucleon and a pion. Our CEM cascade calculation does not include the explicit formation, propagation, and decay of Δ's or any other excited baryons, except by their implicit influence on πN cross sections and scattering and reaction angu-

lar distributions. However, because this is a resonant process with a fairly large cross section, it leads to a very short mean free path for pions with an energy near the resonance energy (~ 180 MeV). The short mean free path leads to a relatively large number of interactions with nucleons before the pion can escape from the nucleus, so that the probability of eventual absorption remains high even with the absorption normalization varying by the factor of 4 mentioned previously. As a somewhat realistic illustration, consider a particle that has a mean free path causing it to interact about 20 times before exiting the nucleus. It still has a high probability of eventual absorption whether absorption is 10% or 40% of the total cross section.

The relativistic quantum molecular dynamics (RQMD 1.08) model [23] does include the possibilities of interferences between collisions and has been used to compute 500 MeV NCX spectra [24], as shown in Fig. 2. This model does less well than that of Gibbs and Kaufmann for the quasielastic peak, and also predicts a self-absorption dip. This reproduction of the relevant feature both classically and quantum mechanically reinforces belief in the validity of the classical transport method used here.

Results of the original Gibbs and Kaufmann INC model are compared to (π^-, π^0) SCX data on carbon at 467 MeV in Fig. 1 by the dashed histograms. This experiment was designed to capture the spectrum at large energy losses, and does not include the quasielastic peak seen in the calculation near 420 MeV at 26°. Just as noted for NCX in Ref. [1], this INC calculation also falls below this SCX data near lab energies of 180 MeV. At 30° and 50°, the INC calculation is lower than the (π^+, π^+) NCX data at a lab energy of 180 MeV by a factor of six. The lower part of the figure also shows the INC calculation lying below the present SCX (π^-, π^0) data by factors of 5 and 4 at 26° and 50°, respec-
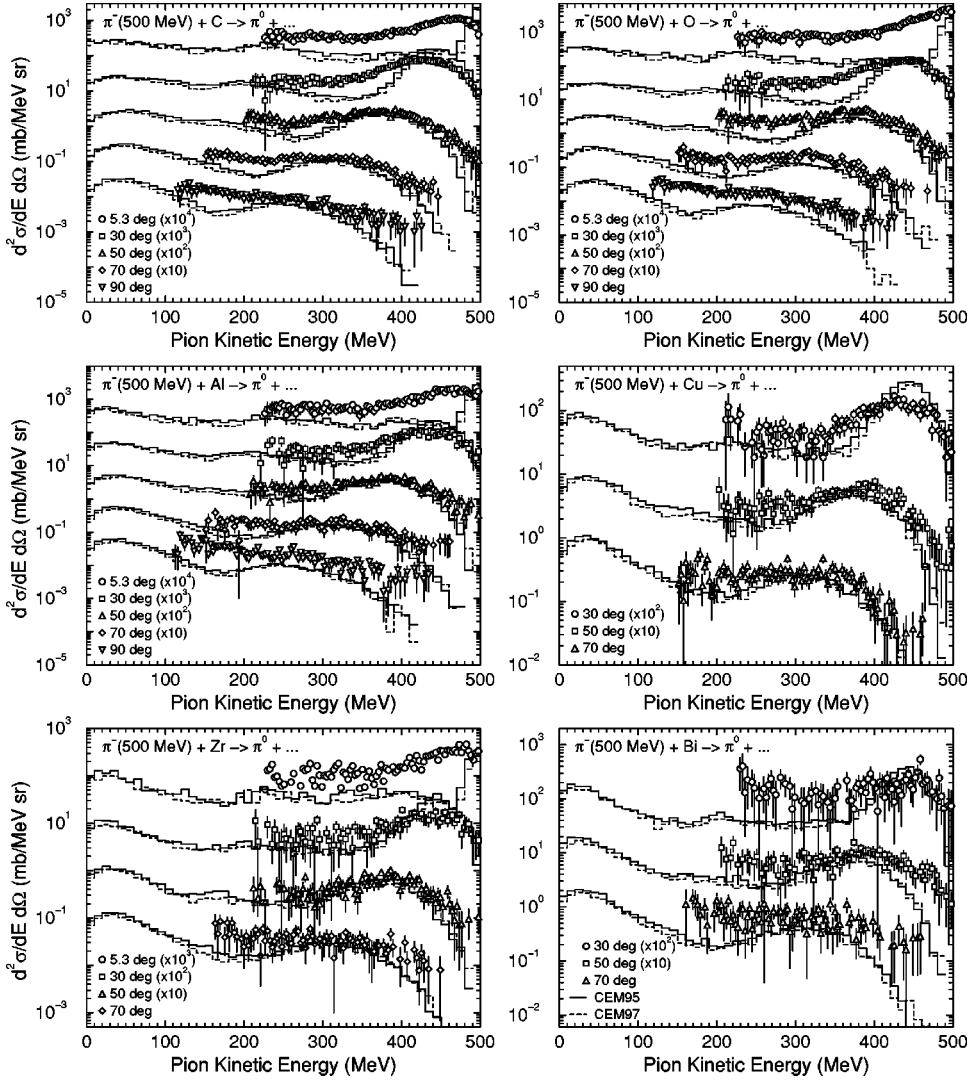
FIG. 5. As in Fig. 4, but using 500 MeV π^- beams [8].

tively. In [1] it is shown that this region of the continuum spectrum is dominated by pions from $(\pi,2\pi)$ reactions.

The heavy solid histograms in the upper part of Fig. 1 show the CEM continuum π^0 spectra for 467 MeV π^- on carbon. At 50° these are near the Gibbs and Kaufmann INC calculations, and a factor of 2 below the data at 180 MeV. At smaller angles the INC histograms are far below the data, while the CEM histograms are low by about a factor of 2.

Also shown in the lower part of Fig. 1 are data and INC calculations for SCX spectra on ^{7}Li. This nucleus has a much lower average density than carbon and heavier nuclei, but shows much the same features in both data and theory seen for carbon.

In Fig. 2 we show the 500 MeV NCX spectra of Zumbro compared to the spectra computed in [1] with the INC code of Gibbs and Kaufmann [2] together with three different CEM calculations and with RQMD results. The CEM99 model yields the thin solid histograms, which show a dip deeper than the dashed histograms at back angles, but agree with the data much better at forward angles. The heavy solid histograms show the RQMD results. As noted in Ref. [1], the self-absorption dip is predicted but not observed for the NCX continuum spectra.

The discrepency between the data and these calculations is present for both the SCX and NCX reaction channels. Application of the Valencia INC model also strongly underestimates the NCX data near 180 MeV [25]. Modifications to gain better agreement with both data sets using the Gibbs and Kaufmann INC model (thin solid histograms in Fig. 1) and the CEM (thin solid histograms in the upper part of Fig. 2) will be descibed in Sec. IV.

Figure 3 shows the contributions to both SCX and NCX pion spectra calculated with the CEM from events with pion production, $(\pi,2\pi)$, compared to the total. One can see that in agreement with [1], the contribution from pion production is also significant in the CEM, both for NCX and SCX pion spectra. Its integral yield (compared to the total) is 24% for NCX at 500 MeV and 47% for SCX at 467 MeV, but these percentages change significantly both with the energy and angle of the detected pions.

The CEM model with different choices of elementary cross sections is compared to 467 MeV SCX spectra for several nuclei in Fig. 4, with essentially the same results. For all cases, the calculations are below the data at 180 MeV, similar to the carbon example in Fig. 1. Figure 5 shows the comparison to SCX spectra from 500 MeV π^- beams on
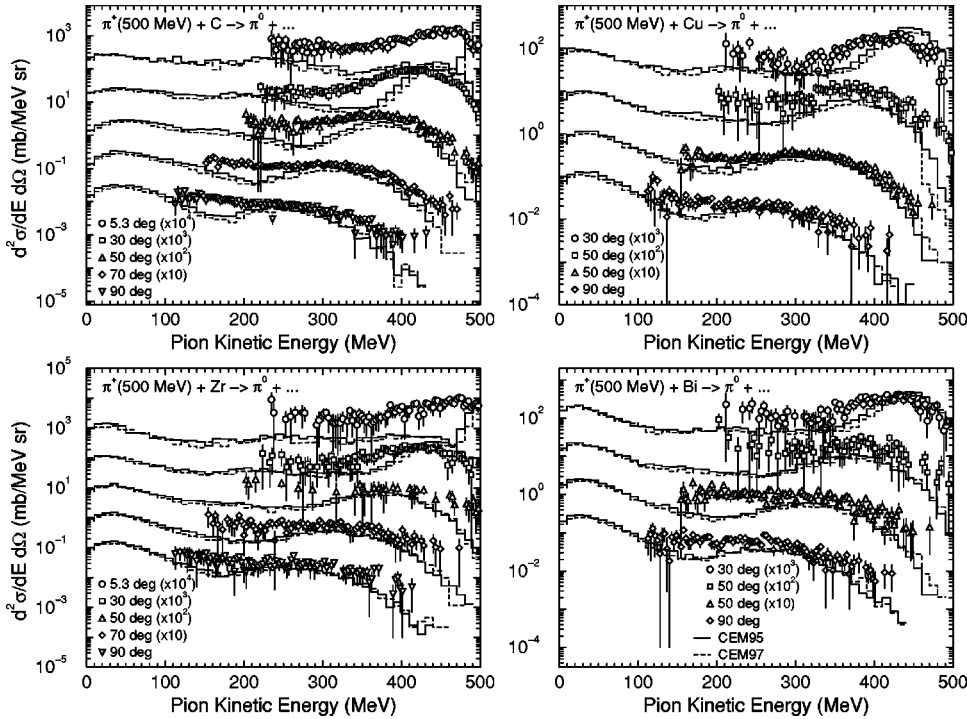
FIG. 6. As in Fig. 4, but using 500 MeV π^+ beams [8].

several targets at several angles. The quasielastic peaks are seen in these spectra, with their general features matched by the CEM histograms, except at the most forward angle (5.3°). At lower lab energies, however, the calculations continue to lie below the data. This is also shown for π^+ projectiles in Fig. 6. With 400 MeV π^-, the same comparison is made at a single reaction angle in Fig. 7. In no case do the calculations agree with the data near 180 MeV.

For nuclei from C through Bi, for three beam energies, and for two reaction models using free-space properties for incoherent cascaded πN and NN interactions, the present SCX analysis agrees with the NCX work of Ref. [1] that something new is needed to prevent the strong role of self-absorption for pions with lab energies near 180 MeV within complex nuclei.

IV. POSSIBLE MEDIUM MODIFICATIONS

In Ref. [1] it was suggested that pions resulting from $(\pi, 2\pi)$ reactions from individual πN collisions within nu-

FIG. 7. As in Fig. 4, but with 400 MeV π^- beams [8].

clei might be forbidden by some rule from interacting with subsequent nucleons for a time of 2 fm/c. Since the outgoing energy spectra near 180 MeV are dominated by produced pions, this had the effect of removing the self-absorption dip and yielding much better agreement with the data. Here we will impose this and two other means to preclude pion reactions within nuclei to seek consistency with the data, which for the SCX spectra include very large nuclei.

In Fig. 1 we show continuum SCX spectra computed with the same code [2] as used for NCX spectra on carbon. The dashed histograms use free-space πN interactions while the light solid ones apply the same 2 fm/c hadronization time for pions from $(\pi, 2\pi)$ reactions used for the NCX calculations in Ref. [1]. This medium-dependent modification accounts for the data, except for some inadequacy at the most forward angle. The NCX spectra do not extend forward of 30°, whereas the π^0 detection scheme readily allows forward angle data. Thus, the same imposed modification in the INC model of Gibbs and Kaufmann makes the same improvement for both NCX and SCX spectra. Figure 1 also shows the same improvement for the case of low-density ^{7}Li.

The Dubna INC code (used in the CEM) tracks particles by distance, not by time as is done in the GK-INC code [2]. Figure 8 compares CEM95 spectra calculated in the standard way (solid histograms) to those with a required propagation distance without interactions of 2 fm for pions resulting from $(\pi, 2\pi)$ reactions (dashed histograms). This modification, analogous to the 2 fm/c hadronization time of Ref. [1], is seen to bring the computed spectra near the data for lab energies near 180 MeV, even for large nuclei, in a fashion similar to that found from the Gibbs and Kaufmann INC. Agreement is especially good for the heavier nuclei.

A mean free path from the CEM is defined as $\lambda = 1/\sigma\rho$, using the local density ρ and free space πN total cross sections σ. The code thus simulates a distribution of λ's, with
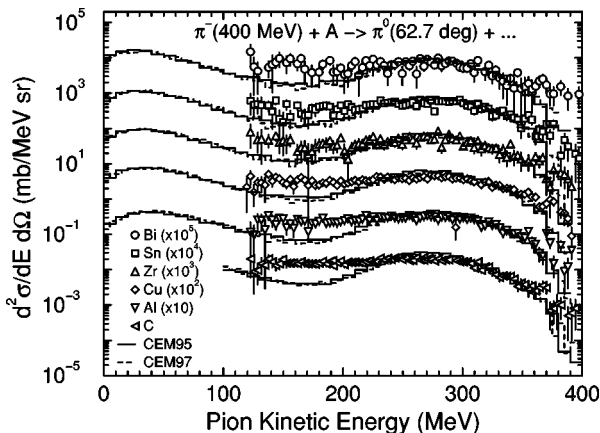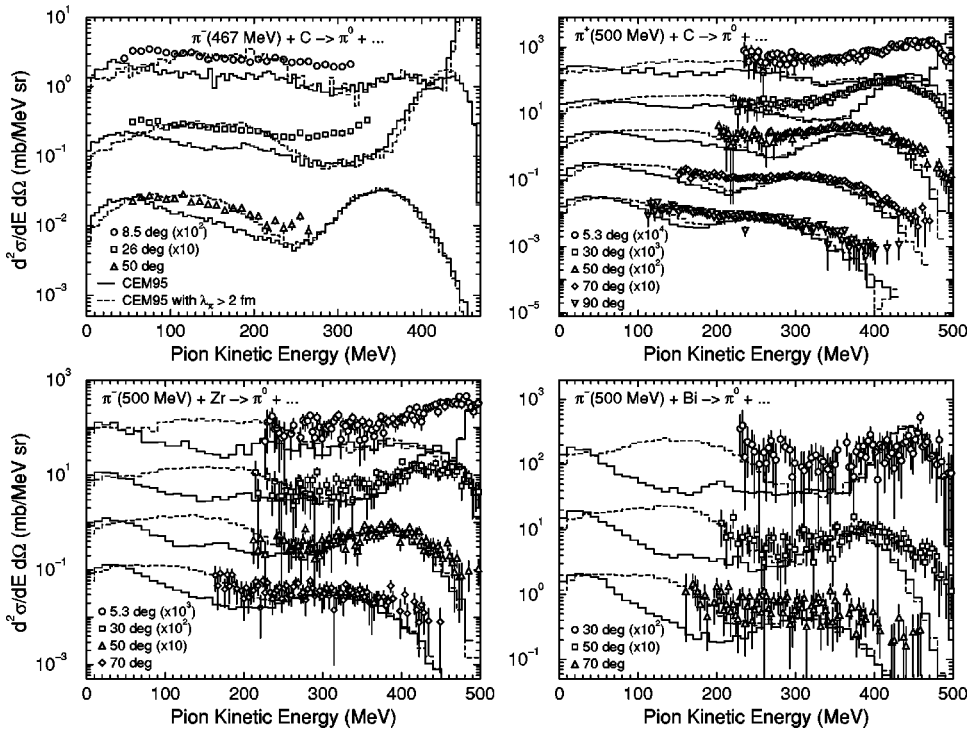
FIG. 8. The effects on π^0 spectra of imposing a condition forbidding pions from ($\pi,2\pi$) reactions from interacting for a distance of 2 fm in the CEM calculations are shown by the dashed histograms, compared to the solid histograms without such effects. For this wide range of nuclear sizes, this medium effect is found to eliminate the self-absorption dip near 180 MeV, matching the trend of the data [7,8].

some larger than the nuclear target but also with many smaller than 1 fm. These small values are not reasonable given the mean internucleon spacing, and are at a length scale inappropriate to the assumption of incoherent scattering inherent in the INC model. Thus another possible medium-dependent modification is to require all pions, not just those resulting from ($\pi,2\pi$) reactions, to travel at least 1.2 fm after their first collision with a nucleon before interacting with another nucleon. (We note that due to much smaller NN cross sections in this energy range and the absence of the absorption of nucleons, the simulated nucleon mean free paths are much longer than those for pions, and a corresponding restriction of them would have a negligible effect on our calculations.) Spectra computed with this effect are shown in Fig. 9. This is seen to suffice for heavy nuclei, with somewhat less success for carbon. Figure 10 shows computed spectra with both the 2 fm minimum path length for pions from ($\pi,2\pi$) reactions and 1.2 fm for all other pions after their first interaction. Agreement here is only slightly better than with only either one of the modifications.

Figures 4–7 show that the discrepancies of the models compared to the measured spectra in the energy region around 180 MeV are approximately the same for all measured nuclei, with perhaps a slight enhancement of the effect for the lighter nuclei. Although a naive expectation might be that the effect should be greater for heavy nuclei, the current simple picture for the transparency effect is consistent with the data. In particular, the idea of restricted interaction for a finite path length will result in a bigger effect for a small nucleus than for a large one.

Medium effects which will permit pions to propagate through nuclei with fewer or weaker interactions than expected from free space cross sections are thus found to provide better agreement with the NCX and SCX continuum spectra. Other tests of the models used and comparisons to other models or to effects that might diminish pion self-absorption in complex nuclei will be discussed in Sec. V.

V. COMPARISONS AND DISCUSSION

A foundation of INC models is classical transport without retaining phase information between collisions. With a central density of 0.16 fm^{-3} giving a mean internucleon spacing of 1.8 fm, this incoherent assumption is valid for a 500 MeV incident beam with a reduced wavelength of 0.3 fm, and for pions in the interesting region near 180 MeV, where the reduced wavelength is 0.7 fm. The model in which we enforce a pion propagation distance greater than 1.2 fm after each πN collision precludes those interactions which come so close together as to violate the classical assumption. The effects of this are shown in Fig. 9. The agreement with the data found there is excellent for heavy nuclei, showing that enforcing the consistency with the assumptions of the INC model may suffice to remove the calculated absorption dip.

Effects of the choice of the earlier [4] relative to the improved [18] version of the πN cross sections are found to be small in the CEM calculations. In the work of Ref. [3] it was found to be too extreme an assumption to allow $\Delta(1232)$ and $N^*(1440)$ decays to be isotropic, while a better modeling of the angular distributions of the decays of these resonant states led to a better reproduction of the data. At forward angles the NCX pion spectra had little sensitivity to this difference, but a proper angular dependence was needed for agreement with back angle data. In the present work it is found that changing the absorption cross sections (quasideuteron absorption) for pions has little effect on the pion spectra (see Sec. III).
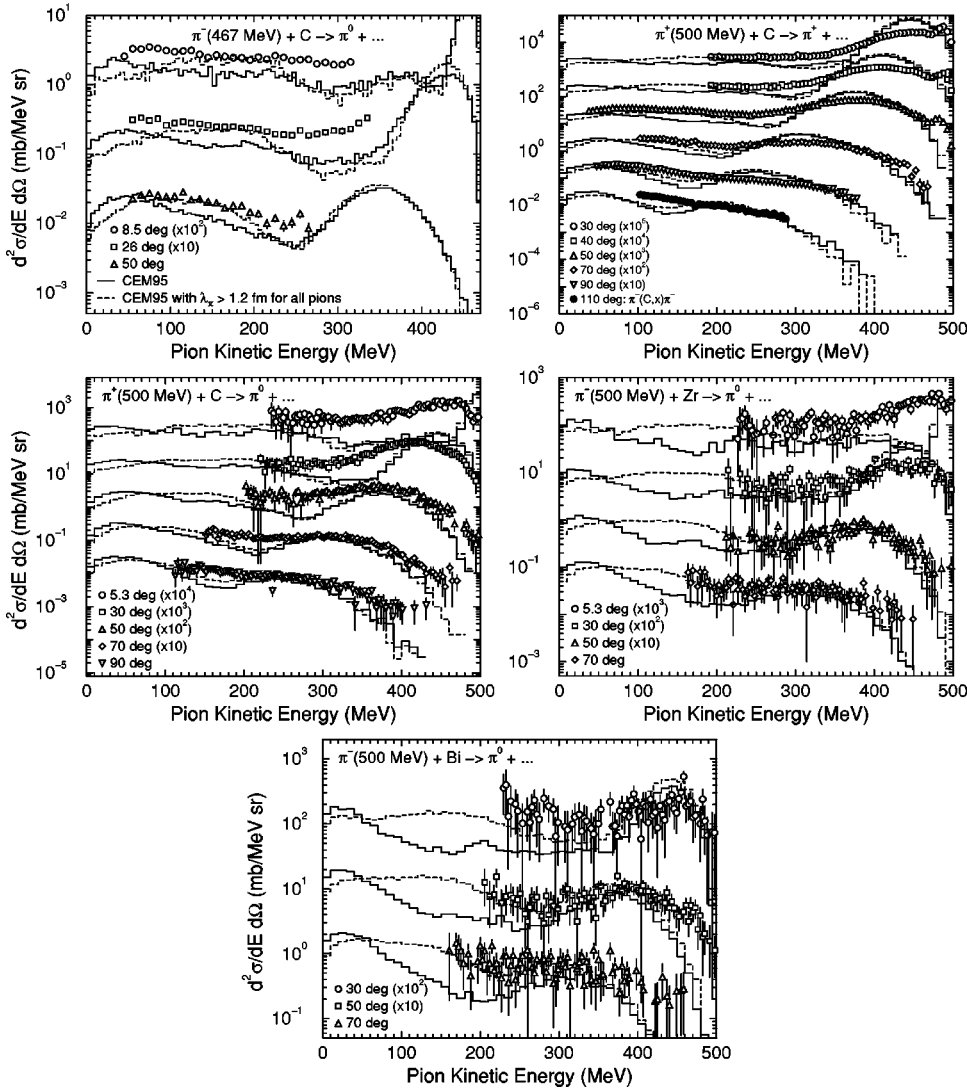
FIG. 9. The effects on π^0 and one set of π^+ spectra of imposing a condition that all pions travel at least 1.2 fm after their first πN interaction before interacting again are shown by the dashed histograms. Comparison to the solid histograms from the standard calculation shows this modification to be successful at filling the self-absorption dip, similar to the results in Fig. 8.

Pion absorption is an important means to provide excitation energy to a nucleus, however, and must influence the spectra of nucleons emitted from nucleon- and pion-induced reactions. Figure 11 shows spectra of nucleons from nucleon-induced reactions [26] (where internal collisons produce pions which may exit or be absorbed), pion-induced nucleon spectra [22,27], and nucleon-induced pion spectra [28]. Nuclear transparency effects, computed in the CEM with both the 2 fm hadronization distance and the 1.2 fm free propagation acting together, decrease yields for nucleon emission spectra by preventing the pion participants from interacting. For pion emission spectra, the nuclear transparency enhances the yields.

Proton-induced pion production data at 730 MeV [28] are in better agreement with the model without medium effects (except at 150°), while pion-induced nucleon spectra [22,27] do not appear to strongly prefer either of the two models (with or without transparency), except at 150°, where the unmodified model does better. Proton-induced neutron spectra [26], where the pions are included but not observed, show somewhat better agreement at more forward angles with the model including transparency, whereas the unmodified

model does better at 120° and 150°. Overall, pion transparency makes the agreement with these data slightly worse.

In the BUU/ART calculations of Ref. [3] it was found that increasing the production of pions by a factor of 3 in ($\pi,2\pi$) reactions could overwhelm the self-absorption process, and give agreement with the data on 500 MeV NCX spectra. Interesting enhancements of ($\pi,2\pi$) spectra have been found for complex nuclei in recent work from TRIUMF [29]. This work also showed pion-induced pion production to occur through independent quasifree scatterings on individual nucleons, with little overall nuclear excitation.

Transport of resonance-energy pions through nuclei without the possibility of pion production can be tested with a 165 MeV π^+ beam [30]. Comparisons to CEM calculations are shown in Fig. 12. The model without transparency effects is seen to do well, indicating that it is indeed the produced pions that are causing the apparent medium effect, while the transport of incident pions in this energy range (below the threshold for the production of additional pions) is successfully modeled by the code. If transparency were due entirely to an incorrect modeling of absorption in this energy range, we would be unable to properly model the propagation of
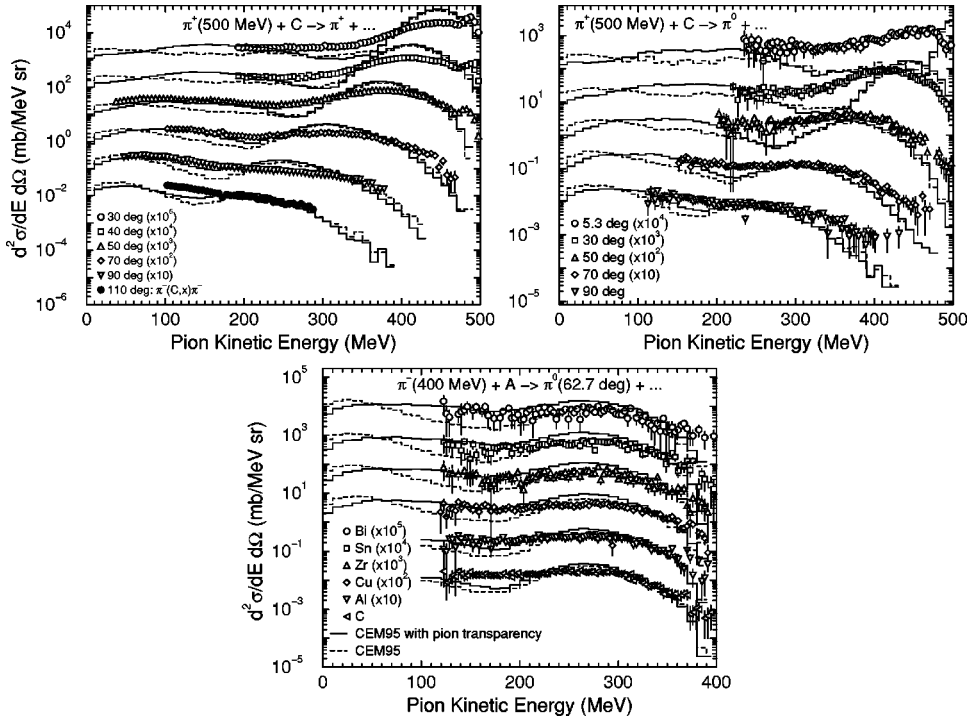
FIG. 10. Application of both medium effects to the CEM calculations shown in Figs. 8 and 9 yields the solid histograms, compared to the dashed histograms without such effects. The combined conditions do not give results significantly different from the use of either one of them alone.

incident pions below the $(\pi,2\pi)$ threshold.

Among the different computational processes used here are two different INC mechanisms, in time [2] or in distance [4]. Similar predictions arise from either version. Effects of pion-nucleus potentials and pion reflections and refractions within the nucleus are found to be of little importance in the CEM model.

Cross sections for low-energy pions are small. This region is below the self-absorption dip, and should be successfully modeled by all techniques. The CEM spectrum in Fig. 1 somewhat underpredicts the SCX yields at forward angles here, while the spectrum using the INC model of Gibbs and Kaufmann matches the data, with or without a hadronization time. CEM calculations agree better with the SCX spectra of Fig. 4, and this region is little changed by including medium effects in that model.

The CEM calculations used in this work do not explicitly include $\Delta(1232)$ and $N^*(1440)$ states, which are known to
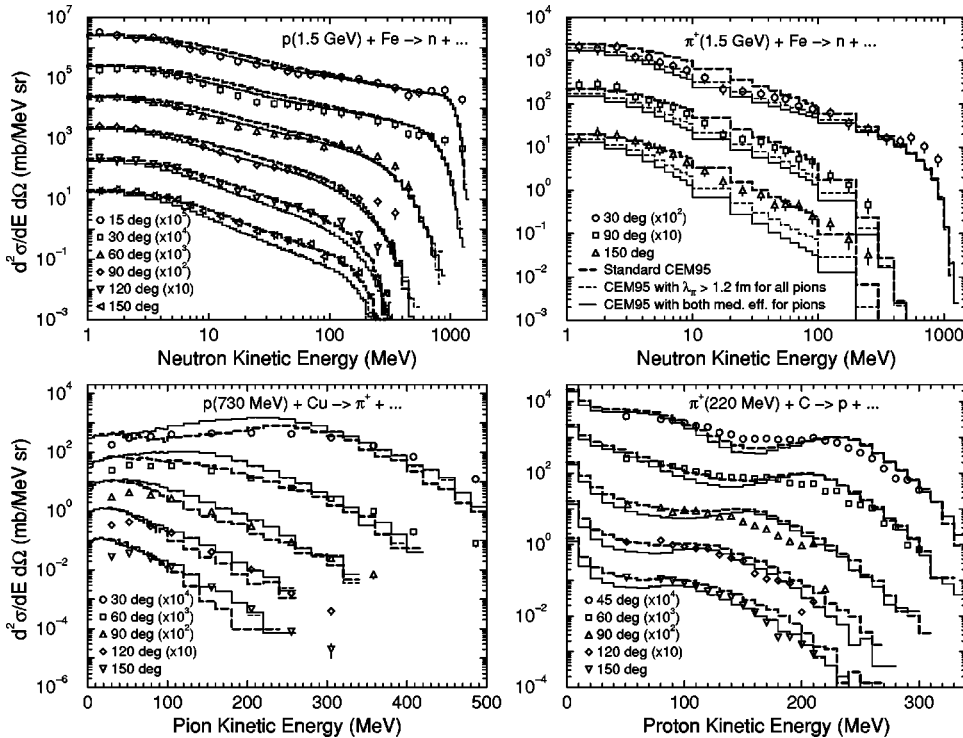

FIG. 11. Application of the full CEM model to reactions including nucleons. The model without medium modifications gives the long-dashed histograms; imposing a condition that all pions travel at least 1.2 fm after their first πN interaction before a subsequent interaction gives the short-dashed histograms; including both transparency effects as used in Fig. 10 gives the solid histograms. Where the short-dashed lines are not visible, they are coincident with the solid lines.
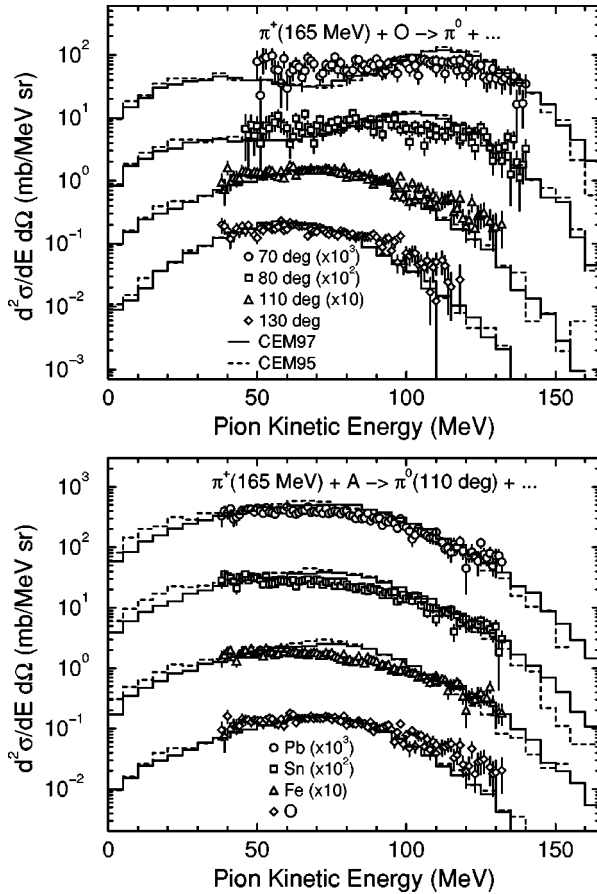
FIG. 12. Inclusive SCX spectra taken with a beam energy of 165 MeV, using the same Pizero Spectrometer used for the present data at higher energies [30], compared to CEM calculated cross sections. The two CEM calculations differ in their approximation to free-space πN cross sections. The agreement found shows that single pions in this energy range are transported correctly by the code without evidence of any pion transparency effects.

be important in heavy-ion induced reactions [31], and were included in the code of Ref. [3]. This may be particularly important near the pion beam energies considered here, atop the $P_{11}(1440)$ which has an important decay branch into the Δ. Transport simulations for heavy-ion reactions that did include Δ and $N*$ participation found only minor effects on the spectra of the emitted pions [31], indicating that the omission of these actors may not be important for the present models of pion continuum spectra.

No correlations between the two pions have been assumed in the present computed spectra. Pion production work has found no evidence for a light isoscalar meson in free space [32], but there is some indication that such a resonance does exist inside nuclei [33]. The great width of this resonance would suggest that it may not be the source of the effects we have modeled, but the predicted strong dependences on the density of matter of its mass and other properties [34] make

it tempting to speculate that this resonance contributes to observed pion transparency effects.

Neutral pion spectra offer a new way to search for correlations among pions, with the possiblity of angular resolution sufficient to use Hanbury-Brown and Twiss (HBT) correlations. The neutral meson spectrometer [35] has excellent angular resolution for emerging photons, which will have readily measured opening angles from each of two neutral pions. Sorting can isolate spectra with two π^0, and their opening angle can be determined. HBT effects from neutral pions will of course be immune to Coulomb distortions and simple to interpret, adding to the spectrum of possiblities recently surveyed [36].

VI. CONCLUSIONS

We have made comparisons of a wide range of SCX and NCX pion continuum spectra to calculations from several semiclassical cascade calculations. All theoretical methods fail to account for the data using only what is known from free-space interactions. One effect that must be included in the nuclear environment is a provision for propagation distances sufficient to maintain the incoherent semiclassical condition between collisions. This is implemented here in the CEM code by imposing a length of 1.2 fm after the first pion-nucleon collision before the next interaction can occur. This is enough to fill the self-absorption dip predicted by the INC codes, and agree with the continuum data quite closely. More exotic medium effects, for instance, a hadronization length of 2 fm before pions from $(\pi,2\pi)$ reactions may again interact, cannot be ruled out, but are not required. Use of the CEM code to predict reaction spectra involving nucleons as well gives predictions that are relatively immune to many of the features of the model, but are overall in slightly worse agreement with backward angle data when the 1.2 fm minimum interaction distance is imposed. These spectra are also sensitive to features of the CEM not used to compute the pion spectra, because they involve the preequilibrium and compound decay portions of the model.

Our present analysis with two different classical cascade models of the pion NCX and SCX data clearly indicates the importance of medium effects for pions to be transported through nuclei. Additional study of these and other related data using better models which explicitly include $\Delta(1232)$, $N*(1440)$, and higher resonances is desirable in order to estimate quantitatively the role of medium effects on pion transport through nuclei.

[1] J. D. Zumbro, C. L. Morris, J. A. McGill, S. J. Seestrom, R. M. Whitton, C. M. Edwards, A. L. Williams, M. R. Braunstein, M. D. Kohler, B. J. Kriss, S. Høibråten, R. J. Peterson, J. Ouyang, J. E. Wise, and W. R. Gibbs, Phys. Rev. Lett. **71**, 1796 (1993).

[2] W. R. Gibbs and W. B. Kaufmann, in *Pion-Nucleus Physics: Future Directions and New Facilities at LAMPF*, Los Alamos, New Mexico, 1987, edited by R. J. Peterson and D. D. Strottman, AIP Conf. Proc. No. 163 (AIP, New York, 1988), p. 279; D. D. Strottman and W. R. Gibbs, Phys. Lett. **149B**, 288 (1984); W. R. Gibbs and J. W. Kruk, Z. Phys. C **46**, S45 (1990).

[3] B.-A. Li, W. Bauer, and C. M. Ko, Phys. Lett. B **382**, 337 (1996).

[4] V. S. Barashenkov and V. D. Toneev, *Interaction of High Energy Particles and Nuclei with Atomic Nuclei* [in Russian] (Atomizdat, Moscow, 1972).

[5] K. K. Gudima, S. G. Mashnik, and V. D. Toneev, Nucl. Phys. **A401**, 329 (1983).

[6] B. L. Clausen, R. A. Loveman, R. J. Peterson, R. A. Ristinen, J. L. Ullmann, and F. Irom, Phys. Rev. C **35**, 1028 (1987).

[7] M. R. Braunstein, Ph.D. thesis, University of Colorado, Los Alamos National Laboratory Report No. LA-12056-T, UC-413 and UC-414, 1991.

[8] J. Ouyang, Ph.D. thesis, University of Colorado; Los Alamos National Laboratory Report No. LA-12457-T, UC-413, 1992.

[9] R. J. Peterson, S. Høibråten, J. Ouyang, M. R. Braunstein, X. Y. Chen, M. D. Kohler, B. J. Kriss, D. J. Mercer, D. S. Oakley, and D. L. Prout, Phys. Lett. B **297**, 238 (1992).

[10] J. D. Bowman, M. D. Cooper, and R. H. Heffner, FORTRAN computer code PIANG, unpublished, described in S. Gilad, Ph. D. thesis, Tel-Aviv University, Tel-Aviv, Israel, 1979.

[11] S. H. Rokni, H. W. Baer, A. G. Bergmann, J. D. Bowman, F. Irom, M. J. Leitch, C. J. Seftor, J. Alster, E. Piasetzky, B. L. Clausen, R. A. Loveman, R. J. Peterson, J. L. Ullmann, J. R. Comfort, J. N. Knudson, and U. Sennhauser, Phys. Lett. B **202**, 35 (1988).

[12] R. A. Arndt and L. D. Roper, program SAID (Scattering Analysis Interactive Dial-in), Report No. CAPS-80-3 (rev.), Center for Analysis of Particle Scattering, Virginia Polytechnic Institute and State University, Blacksburg, Virginia (1983); R. A. Arndt, J. M. Ford, and L. D. Roper, Phys. Rev. D **32**, 1085 (1985).

[13] J. Ouyang, S. Høibråten, and R. J. Peterson, Phys. Rev. C **47**, 2809 (1993).

[14] J. Ouyang, S. Høibråten, and R. J. Peterson, Phys. Rev. C **48**, 1074 (1993).

[15] S. G. Mashnik, A. J. Sierk, O. Bersillon, and T. A. Gabriel, Nucl. Instrum. Methods Phys. Res. A **414**, 68 (1998); Los Alamos National Laboratory Report No. LA-UR-2905 (1997); http://t2.lanl.gov/publications/publications.html

[16] M. Blann, H. Gruppelar, P. Nagel, and J. Rodens, *International Code Comparison for Intermediate Energy Nuclear Data* (NEA OECD, Paris, 1994).

[17] S. G. Mashnik, Acta Phys. Pol. B **24**, 1685 (1993); Rev. Roum. Phys. **37**, 179 (1992); Yad. Fiz. **58**, 1772 (1995) [Phys. At. Nucl. **58**, 1672 (1995)].

[18] S. G. Mashnik and A. J. Sierk, ''Improved Cascade-Exciton Model of Nuclear Reactions,'' Los Alamos National Laboratory Report No. LA-UR-98-5999 (1998); http://xxx.lanl.gov/ps/nucl-th/9812069; *Proceedings of the Fourth Workshop on Simulating Accelerator Radiation Environments (SARE-4)*, Knoxville, TN, 1998, edited by Tony A. Gabriel (ORNL, 1999), p. 29.

[19] A. S. Iljinov, *Code for Calculation of Intranuclear Cascades at Energies* $T \leqslant 5$ *GeV* [in Russian], Joint Institute for Nuclear Research Report No. B1-4-5478, Dubna, 1970.

[20] S. G. Mashnik, Nucl. Phys. **A568**, 703 (1994).

[21] H. J. Weyer, Phys. Rep. **195**, 295 (1990).

[22] R. D. McKeown, S. J. Sanders, J. P. Schiffer, H. E. Jackson, M. Paul, J. R. Specht, E. J. Stephenson, R. P. Redwine, and R. E. Segel, Phys. Rev. Lett. **44**, 1033 (1980); Phys. Rev. C **24**, 211 (1981); tabulated data of measurements are published in AIP Document No. PAPS PRVCA-24-211-48.

[23] H. Sorge, H. Stöcker, and W. Greiner, Ann. Phys. (N.Y.) **192**, 266 (1989), and references therein.

[24] C. L. Morris and J. D. Zumbro, in *Proceedings of the International Conference on Mesons and Nuclei at Intermediate Energies, Dubna, Russia, 1994*, edited by M. Kh. Khankhasayev and Zh. B. Kurmanov (World Scientific, Singapore, 1995), p. 271.

[25] M. J. Vicente-Vacas, M. Kh. Khankhasayev, and S. G. Mashnik, ''Inclusive Pion Double-Charge-Exchange Above 0.5 GeV,'' University of Valencia Preprint No. FTUV/94-73 1994; http://xxx.lanl.gov/ps/nucl-th/9412023 v2.

[26] K. Ishibashi, H. Takada, T. Nakamoto, N. Shigyo, K. Maehata, N. Matsufuji, S. Meigo, S. Chiba, M. Numajiri, Y. Watanabe, and T. Nakamura, J. Nucl. Sci. Technol. **34**, 529 (1997).

[27] T. Nakamoto, K. Ishibashi, N. Matsufuji, N. Shigyo, K. Maehata, H. Arima, S. Meigo, H. Takada, S. Chiba, and M. Numajiri, J. Nucl. Sci. Technol. **34**, 860 (1997).

[28] D. R. F. Cochran, P. N. Dean, P. A. M. Gram, E. A. Knapp, E. R. Martin, D. E. Nagle, R. B. Perkins, W. J. Shlaer, H. A. Thiessen, and E. D. Theriot, Phys. Rev. C **6**, 3085 (1972); Los Alamos Scientific Laboratory Report No. LA-5083-MS, Los Alamos, 1972.

[29] F. Bonutti, P. Camerini, E. Fragiacomo, N. Grion, R. Rui, J. T. Brack, L. Felawka, E. F. Gibson, G. Hofman, M. Kermani, E. L. Mathie, S. McFarland, R. Meier, D. Ottewell, K. Raywood, M. E. Sevior, G. R. Smith, and R. Tacik, Phys. Rev. C **55**, 2998 (1997).

[30] S. Høibråten, Ph.D. thesis, Massachusetts Institute of Technology; Los Alamos National Report No. LA-11582-T, UC-414, 1989; J. E. Wise, M. R. Braunstein, S. Høibråten, M. D. Kohler, B. J. Kriss, J. Ouyang, R. J. Peterson, J. A. McGill, C. L. Morris, S. J. Seestrom, R. M. Whitton, J. D. Zumbro, C. M. Edwards, and A. L. Williams, Phys. Rev. C **48**, 1840 (1993).

[31] J. Helgesson and J. Randrup, Phys. Lett. B **439**, 243 (1998).

[32] F. Bonutti, P. Camerini, E. Fragiacomo, N. Grion, R. Rui, J. T. Brack, L. Felawka, E. F. Gibson, G. Hofman, M. Kermani, E. L. Mathie, S. McFarland, R. Meier, K. Raywood, D. Ottewell, M. E. Sevior, G. R. Smith, R. Tacik, and M. Vicente-Vacas, Nucl. Phys. **A638**, 729 (1998).

[33] F. Bonutti, P. Camerini, E. Fragiacomo, N. Grion, R. Rui, J. T. Brack, L. Felawka, E. F. Gibson, G. Hofman, M. Kermani, E. L. Mathie, S. McFarland, R. Meier, K. Raywood, D. Ottewell, M. E. Sevior, G. R. Smith, and R. Tacik, Phys. Rev. C **60**, 018201 (1999).

[34] K. Saito, K. Tsushima, A. W. Thomas, and A. G. Williams, Phys. Lett. B **433**, 243 (1998).

[35] H. W. Baer, R. D. Bolton, J. D. Bowman, M. D. Cooper, F. H. Cverna, R. H. Heffner, C. M. Hoffman, N. S. P. King, J. Piffaretti, J. Alster, A. Doron, S. Gilad, M. A. Moinester, P. R. Bevington, and E. Winkelmann, Nucl. Instrum. Methods **180**, 445 (1981); S. Gilad, Ph. D. thesis, Tel-Aviv University, 1979.

[36] A. Z. Mekjian, B. R. Schlei, and D. Strottman, Phys. Rev. C **58**, 3627 (1998).